



Cite this: RSC Adv., 2015, 5, 59912

## Application of a tailor-made polymer as a selective and sensitive colorimetric sensor for reliable detection of trace levels of uranyl ions in complex matrices†

Mohammad Behbahani,<sup>\*a</sup> Sara Salimi,<sup>a</sup> Hamid Sadeghi Abandansari,<sup>a</sup> Fariborz Omidi,<sup>b</sup> Mani Salarian<sup>c</sup> and Ali Esrafil<sup>d</sup>

In this study, a new colorimetric chemosensor based on ion imprinted polymer nanoparticles was designed for quantitative detection of uranyl ions at trace levels in environmental water samples. The removal and pre-concentration of uranyl ions using the synthesized imprinted polymer was performed under optimized conditions and the color of the sorbent changed from yellow to violet.  $\text{UO}_2^{2+}$ -imprinted polymer nanoparticles were synthesized by a precipitation polymerization technique. The sorbent was characterized using solid state UV-vis analysis, thermogravimetric analysis (TGA), differential thermal analysis (DTA), scanning electron microscopy (SEM), elemental analysis (CHN) and Fourier transform infrared spectrometry (FT-IR). The color change provides a simple, rapid and reliable method for the sensitive and selective visual detection of trace levels of uranyl ions without the need of sophisticated instruments. The color of the sorbent in the absence and presence of uranyl ions shifts from yellow to violet. The method detection limit of the synthesized chemo-sensor for uranyl ions was 0.0005 ppm. The method was successfully applied for trace detection of uranyl ions in distilled, tap, Caspian Sea and Persian Gulf water samples.

Received 17th May 2015  
Accepted 1st July 2015

DOI: 10.1039/c5ra09221c  
[www.rsc.org/advances](http://www.rsc.org/advances)

### 1. Introduction

Uranium is a radioactive element which exists naturally in the environment.<sup>1</sup> Nowadays, the risk of exposure to uranium causing adverse effects to human health has been increased tremendously,<sup>2,3</sup> uranium is one of the main sources in nuclear energy generation and enriched uranium is a major component in nuclear weapons. Uranium has many forms in aqueous solution, and the most soluble or bioavailable form is uranyl ( $\text{UO}_2^{2+}$ ). The maximum contamination level of  $\text{UO}_2^{2+}$  in drinking water is defined as  $1.30 \times 10^{-7}$  mol L<sup>-1</sup> by the U.S. Environmental Protection Agency (EPA),<sup>4</sup> therefore, it is desirable to have simple and convenient analytical methods that can determine the uranyl present in the aqueous medium at trace levels. Many analytical techniques, require expensive and

complicated instruments such as inductively coupled plasma-mass spectrometry (ICP-MS),<sup>5–7</sup> and atomic absorption spectrometry<sup>8,9</sup> which makes onsite real-time sensing difficult. Optical sensing approaches (e.g. laser fluorimetry,<sup>10,11</sup> absorption,<sup>12,13</sup> luminescence<sup>14</sup>) and electrochemical approaches<sup>15,16</sup> for the detection of environmental and biological uranium have been developed in the field of chemical sensors across several decades. Among the optical sensors, the fluorescence-based technique is a very appealing approach for future practical application due to its intrinsic sensitivity and high spatial resolution.<sup>17,18</sup> For instance, Ganesh *et al.* reported the determination of the uranium concentration in a raffinate stream of the Purex process during reprocessing of spent nuclear fuel using fluorescence enhancing reagents such as sodium pyrophosphate;<sup>19</sup> Angel *et al.* reported the detection of uranyl ion *via* fluorescence quenching and photochemical oxidation of calcein with the detection limit of  $4.0 \times 10^{-8}$  mol L<sup>-1</sup>,<sup>20</sup> recently Liao *et al.* described the separation and determination of trace uranium using a double-receptors method based on immobilized salophen and fluorescence labeled oligonucleotide.<sup>21</sup> However, these methods always require additional chemicals (such as sodium pyrophosphate, calcein and oligonucleotide) or devices (such as balllens<sup>22</sup>) to obtain high sensitivity and high selectivity. Recently we noticed the fluorescence-signaling DNA aptamers and deoxyribozymes were used as novel biosensing

<sup>a</sup>Department of Chemistry, Shahid Beheshti University, Tehran, Iran. E-mail: mohammadbehbahani89@yahoo.com; Fax: +98 2122431683, +98 411333458; Tel: +98 2122431661, +98 9141028230

<sup>b</sup>Department of Occupational Health Engineering, School of Public Health, Shahrood University of Medical Sciences, Shahrood, Iran

<sup>c</sup>Department of Chemistry, Georgia State University, Atlanta, Georgia, USA

<sup>d</sup>Department of Environmental Health Engineering, School of Public Health, Iran University of Medical Sciences, Tehran, Iran

† Electronic supplementary information (ESI) available. See DOI: 10.1039/c5ra09221c

moieties for heavy metal ions.<sup>23–25</sup> For example, Lu *et al.* reported a catalytic beacon sensor for  $\text{UO}_2^{2+}$  based on an *in vitro* selected  $\text{UO}_2^{2+}$  specific DNAzyme, and this method has a 45 pM detection limit and million-fold selectivity.<sup>26</sup> However, such biosensors (uranyl-specific DNAzyme) is costly due to the complication of *in vitro*-selection. Therefore, there is still an urgent need to develop new simple and convenient methods with high sensitivity and high selectivity for the detection of trace uranium in the environment.

Based on the idea of molecular imprinting technique, ion-imprinted polymers (IIPs) have attracted much attention as selective sorbents for preconcentration of metal ions.<sup>27</sup> In ion imprinting techniques, the ion-ligand complex serves as a template. In ion imprinting process, three general steps are applied, which include the complexation of metal ion with a suitable ligand (formation of template) as the initial step. The second step is the co-polymerization of monomers in the presence of template, and afterwards removal of complex from the polymer. For adsorption of the target ion, the prepared polymer was put into a solution containing metal ions. Ion-imprinted polymers have various applications, *e.g.* in separation, preconcentration and purification processes with regard to metal ions including transition elements,<sup>28</sup> actinides,<sup>29</sup> lanthanides,<sup>30</sup> and noble metals in diverse matrices.<sup>31</sup>

In this work, the ion imprinted polymer nanoparticles were applied as a highly selective and sensitive colorimetric sensor for visual detection of ultra-trace levels of uranyl ions in aqueous solution. The nanosized  $\text{UO}_2^{2+}$ -imprinted polymer was prepared by precipitation polymerization technique.

The parameters affecting the visual detection of uranyl ions were investigated and optimized. In these experimental conditions, when the synthesized imprinted polymer nanoparticles interact with uranyl ions, a color change from yellow to violet can be observed. The high sensitivity of the sensor enables the qualitative detection of uranyl ions at trace levels. The method detection limit of the sensor for uranyl ions was 0.0005 ppm.

## 2. Experimental

### 2.1. Reagents and materials

Methacrylic acid (MAA) and 2-(5-bromo-2-pyridylazo)-5-(diethylamino) phenol (Br-PADAP) with high purity was purchased from Merck (Darmstadt, Germany, <http://www.merck.de>). Ethylene glycol dimethacrylate (EGDMA) was obtained from Fluka (Buchs SG, Switzerland, <http://www.sigmaaldrich.com>). 2,2'-Azobisisobutyronitrile (AIBN) was obtained from Acros Organics (New Jersey, USA). NaOH, HCl,  $\text{HNO}_3$ , acetonitrile and methanol were purchased from Merck (Darmstadt, Germany). All other reagents used in this study were of analytical grade and purchased from Merck (Darmstadt, Germany, <http://www.merck.de>). Stock solutions of  $\text{UO}_2^{2+}$ ,  $\text{Cr}^{2+}$ ,  $\text{Cd}^{2+}$ ,  $\text{Pd}^{2+}$ ,  $\text{Zn}^{2+}$ ,  $\text{Ni}^{2+}$ ,  $\text{Ca}^{2+}$ ,  $\text{Mg}^{2+}$ ,  $\text{Ag}^+$ ,  $\text{Fe}^{3+}$ ,  $\text{Mn}^{2+}$ ,  $\text{Na}^+$ ,  $\text{K}^+$  and  $\text{Co}^{2+}$  were prepared with the addition of an appropriate amount of nitrate salts in ultra-pure water. Ultra-pure water was prepared using a Milli-Q system from Millipore (Bedford, MA, USA).

### 2.2. Apparatus

A digital pH meter, Metrohm 827 Ion analyzer (Herisau, Switzerland), equipped with a combined glass calomel electrode was used for the pH adjustments at  $25 \pm 1$  °C temperature. Heidolph heater stirrer model MR 3001 (Germany) was employed for heating and stirring of the solutions. Fourier transform infrared (FT-IR) spectra ( $4000\text{--}200\text{ cm}^{-1}$ ) in KBr were recorded using Bruker IFS66/S FT-IR spectrometer. The CHN analysis was performed on a Thermo Finnigan Flash EA112 elemental analyzer (Okehampton, UK). Scanning electron microscopy (SEM) was performed by gently distributing the powder sample on the stainless steel stubs, using SEM (KYKY, EM3200) instrument. The thermal properties of synthesized polymers were determined using a BAHR-Thermoanalyse GmbH (Germany) with employing, heating and cooling rates of  $10\text{ }^\circ\text{C min}^{-1}$  and using a condenser as the coolant. The samples were weighed as a thin film and carefully packed into a clean aluminum pan (11.5–12.5 mg), and sealed by crimping an aluminum lid on the pan (Shimadzu universal crimper). An  $\text{Al}_2\text{O}_3$  empty pan sealed with a cover pan was used as a reference sample. A scanning range of 10 to  $800\text{ }^\circ\text{C}$  was used for samples at  $10\text{ }^\circ\text{C min}^{-1}$  in nitrogen gas. The reflection spectra of the chemosensor were collected using a solid state 2100-UV-vis Shimadzu spectrophotometer.

### 2.3. Synthesis of $\text{UO}_2^{2+}$ ion imprinted polymer nanoparticles

The nanosized  $\text{UO}_2^{2+}$ -imprinted polymer was prepared by precipitation polymerization technique. In the first step, 2 mmol of methacrylic acid (functional monomer) and 2 mmol of 2-(5-bromo-2-pyridylazo)-5-(diethylamino)phenol (the uranyl-binding ligand) were dissolved in 100 mL of acetonitrile/methanol (1 : 1 v/v) in a 200 mL glass flask. Subsequently, as the second step, 1 mmol of  $\text{UO}_2(\text{NO}_3)_2$  as an imprinted metal ion (template) was added slowly to a glass flask and the resulted mixture was stirred for 5 h at room temperature. In the third step, 16 mmol of EGDMA and 100 mg of AIBN were added as cross-linker and initiator. The oxygen of the sample solution was removed by bubbling nitrogen through the sample for 10.0 min. Polymerization was performed in an oil bath at  $65\text{ }^\circ\text{C}$  for 24 h in the presence of nitrogen under magnetic stirring at 400 rpm. The prepared polymer was washed several times with 1 : 4 (v/v) methanol/water to remove the unreacted materials and then with HCl (1.0 mol L<sup>-1</sup>) for leaching the imprinted metal ions (uranyl ions) until the washing solution was free from uranyl ions. Finally, it was washed with double distilled water until reached a neutral pH (Fig. 1 provides the images of synthesized nanosized IIP after each step).

### 2.4. Naked-eye colorimetric detection of uranyl ions

Batch experiments were used for investigation of factors in visual detection of target ion. In the pre-concentration and visual detection step, the pH of sample solution was adjusted to 7.0 by drop wise addition of 2 mol L<sup>-1</sup> sodium hydroxide or hydrochloric acid solutions. Then, 10 mg of dried polymer was suspended in aqueous solution containing specific amount of

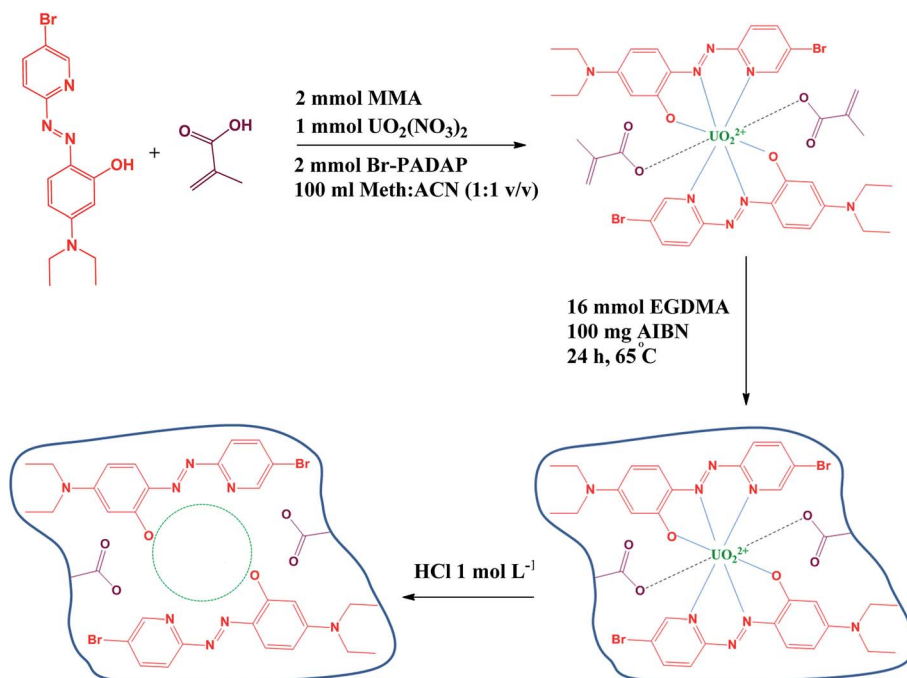


**Fig. 1** Schematic illustration of imprinting process for the preparation of uranyl-imprinted polymer nanoparticles by precipitation polymerization technique.

$\text{UO}_2^{2+}$  and stirred for 5 minutes with a magnetic stirrer. Fig. 2 displays the naked-eye colorimetric change of the imprinted polymer with (1 ppm of uranyl ion). Using the proposed chemosensor, uranyl ions can be pre-concentrated and then visually detected over a wide range [(0.001–100 ppm)]. Fig. 2 demonstrates a selective color change from yellow to violet. The color change provides a simple, rapid and reliable method for the sensitive and selective detection of trace levels of uranyl ions without the need for sophisticated instruments.

### 2.5. Real sample pretreatment

The tested water samples were distilled water, tap water (Tehran, Iran), and sea water (Persian Gulf and Caspian Sea). The sea water samples were collected in polyethylene bottles. They were cleaned with acid bath, and then filtered through nylon filters (Millipore, 0.22  $\mu\text{m}$ ) before the analysis. Finally, the pH of each solution was adjusted to 7.0 by drop wise addition of HCl and NaOH for separation and visual detection of uranyl ions from the water samples.

## 3. Results and discussion

### 3.1. Characterization of the chemosensor

**3.1.1. Solid state UV-vis analysis.** The solutions with 1 ppm concentration of  $\text{UO}_2^{2+}$  ions were prepared by dissolving specific amounts of  $\text{UO}_2(\text{NO}_3)_2$  in distilled water. Then 10 mg of synthesized sorbent was immersed into  $\text{UO}_2^{2+}$  aqueous solution and stirred for 5 min. The formation of complex between Br-PADAP and uranyl ions is violet color. The color of the sorbents changed quickly from yellow to violet and determined

by naked eye (Fig. 2) and UV-vis spectrophotometer. According to the obtained data by UV-vis spectrometer, the maximum reflectance spectra of the imprinted polymer ( $453 \text{ cm}^{-1}$ ) shifted to higher wavelength values ( $584 \text{ cm}^{-1}$ ) in the presence of uranyl ions which can prove the selective color change of the proposed chemosensor in the presence of uranyl ions.

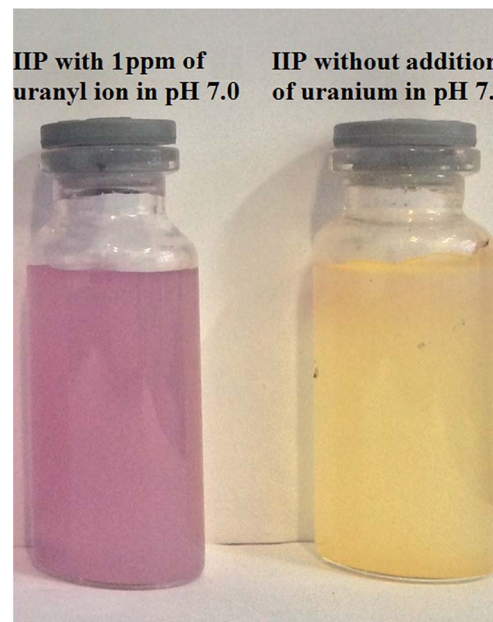


**Fig. 2** Selective color change of ion imprinted polymer nanoparticles from yellow to violet in the presence of uranyl ions.

Generally, the electrostatic interaction of a bound metal ion would not be able to produce such pronounced effects on the electronic structure of a dye molecule, and hence its spectrum. It seems reasonable that a large change in the conjugation system (longer conjugation system) of Br-PADAP molecule upon uranyl ion complexation is causing the observed effect. The aim of this work was to synthesize a tailor-made polymer for selective pre-concentration and trace detection of uranyl ions in presence of potentially interfering ions. In the other hand, when we synthesize IIP with cross linking of target complex (complex between Br-PADAP and uranyl ions), the violet color of Br-PADAP and uranyl ions complex was selectively and visually detectable in the presence of potentially interfering ions in complex matrices such as sea water samples.

**3.1.2. FT-IR analysis.** FTIR spectra of unleached-IIP and leached-IIP are given in Fig. 3. The spectra of unleached-IIP and leached-IIP illustrate vibration bands of OH ( $3450\text{ cm}^{-1}$ ), N=N ( $1391\text{ cm}^{-1}$ ) and C=N ( $1650\text{ cm}^{-1}$ ) which further confirm the presence of Br-PADAP in the polymer bead. The peak appeared at  $1650\text{ cm}^{-1}$  corresponding to C=N stretching vibration for Br-PADAP was shifted to  $1639\text{ cm}^{-1}$  for unleached IIP. In addition, the peak appeared at  $1391\text{ cm}^{-1}$  due to N=N stretching vibration of Br-PADAP was shifted to  $1378\text{ cm}^{-1}$  for unleached IIP. The decrease in band frequencies indicates that the uranyl ions have been coordinated with non-bonding electron pairs of nitrogen in Br-PADAP, and as a result, it demonstrates the presence of uranyl ions in unleached IIP structure. On the other hand, the broad band which observed at  $3450\text{ cm}^{-1}$  is attributed to O-H stretching vibration of hydroxyl group from Br-PADAP. The shift obtained for this band in unleached IIP to  $3390\text{ cm}^{-1}$  is due to hydroxyl group of Br-PADAP involved in the interaction.

**3.1.3. SEM images.** The morphology of the  $\text{UO}_2^{2+}$ -IIP was assessed by scanning electron microscopy, and the SEM micrograph is shown in Fig. 4. The SEM pattern showed particles with the size of about 25–50 nm. As a result,  $\text{UO}_2^{2+}$ -IIP can be used as a nano-size selective solid phase for very fast pre-concentration and trace visual detection of uranyl ions.

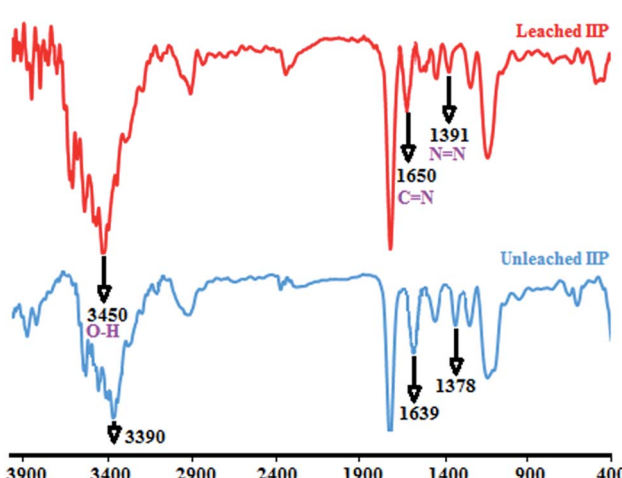


Fig. 3 The FT-IR spectra of leached and unleached uranyl-imprinted polymer nanoparticles.

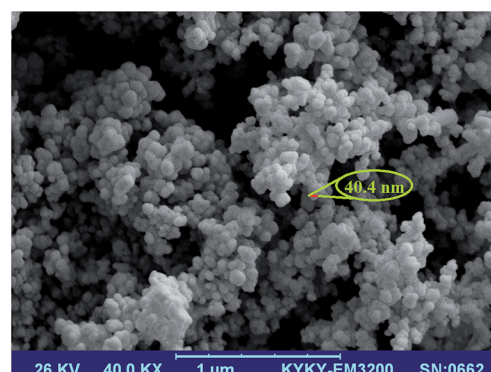


Fig. 4 The SEM image of uranyl-imprinted polymer nanoparticles.

**3.1.4. Thermogravimetry (TG) analysis.** Thermal stability of the leached (the imprinted polymer washed with optimized elution solvent and free from target ions) and unleached (the imprinted polymer with the target ions sorbed in the synthesized imprinted polymer) imprinted polymer was evaluated by TGA. Fig. 5(a) show TGA plots for leached and unleached ion imprinted polymer. As it is shown in TG plot for unleached ion imprinted polymer, weight loss for  $\text{UO}_2^{2+}$ -IIP was about 82%, and this amount of reduction in weight is related to the presence of uranyl ions in polymer bead. While decrease in weight for leached imprinted polymer up to 100%, is due to the

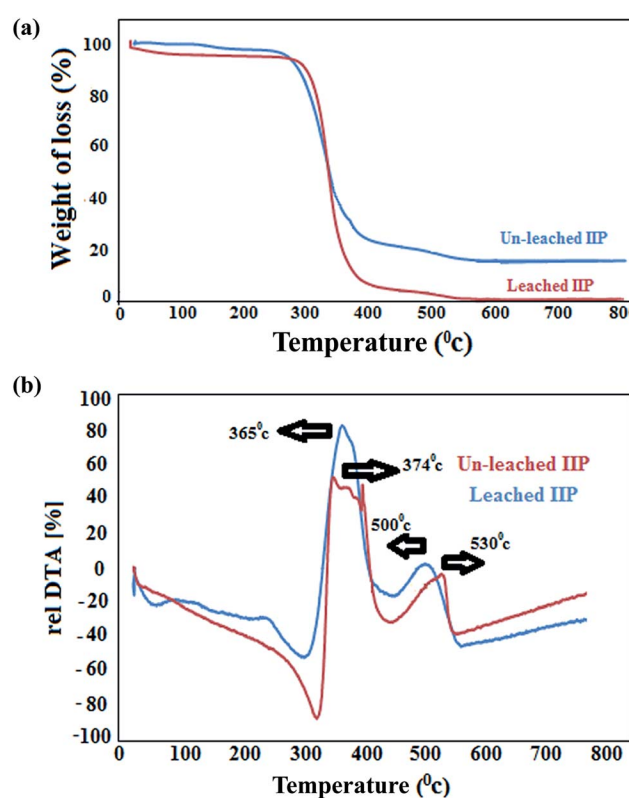


Fig. 5 (a) TGA plot of leached and unleached uranyl-imprinted polymer nanoparticles (b) DTA plot of leached and unleached uranyl-imprinted polymer nanoparticles.

absence of uranyl ions in polymer. These observations indicate that the formation of  $\text{UO}_2^{2+}$ -imprinted polymer and elution of uranyl ions from the polymer was performed successfully.

**3.1.5. Differential thermal analysis (DTA).** Fig. 5(b) shows DTA plots for leached and unleached imprinted polymer. In DTA plots of uranyl imprinted polymer, exothermic peaks were observed at 374 and 530 °C (for unleached) and 365 and 500 °C (for leached). As can be seen in the DTA plots, the temperature at maximum peaks in  $\text{UO}_2^{2+}$ -IIP was observed at higher temperature of 374 and 530 °C; while for the leached-IIP, it is observed in the lower temperature of 365 and 500 °C. These observations confirm the higher thermal stability of the unleached compared to leached polymer, which is due to the presence of uranyl ions in the un-leached polymer and also its strong complexation with Br-PADAP in the polymeric network.

**3.1.6. Elemental analysis.** The results of elemental analysis (EA) of acid leached IIPs were found to be: (% found); C, (55.87%); H, (7.2%) and N, (1.282%). These observations confirm the successful immobilization of ligand in imprinted polymer nanoparticles.

### 3.2. Naked-eye colorimetric optimization

**3.2.1. Effect of pH.** The high efficiency of the visual sensor depends on key factors such as contact-time (signal response time) and pH of solution. These key factors forcefully affect the homogeneity in the color map repartition and intensity even at low loading level of ions during visual detection. The efficiency of metal ion-sensing with colorimetric sensor was considerably influenced by the pH of the solution (Fig. 6). As can be seen in the Fig. 6, the maximum color intensity of uranyl ions by the synthesized ion imprinted polymer nanoparticles was achieved in the pH of 7.0. Therefore, pH of 7.0 was chosen as the optimum pH for next experiments.

**3.2.2. Response time.** An important colorimetric detection feature of any chemo-sensor is its response time. The response time of the present chemo-sensor is controlled by the time required for ions to diffuse from the aqueous solution to the sorbent and create a high color change for simple visual detection of target ions (Fig. 7). For the detection of the response time, solutions with 1 ppm concentration of uranyl ions were prepared by dissolving  $\text{UO}_2(\text{NO}_3)_2$  in the distilled water. After pH adjustment (pH of 7.0), 10 mg of sorbent was

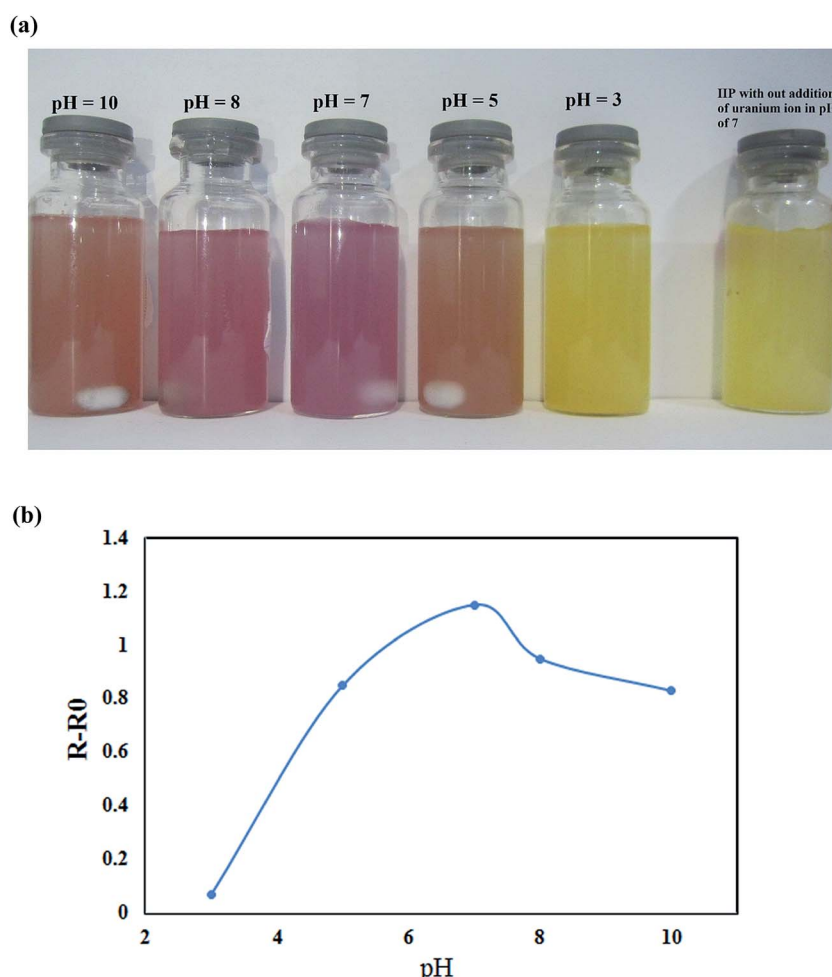


Fig. 6 Influence of pH of the ions solution on the visual detection of uranyl ions. Condition: response time, 5 min; concentration of  $\text{UO}_2^{2+}$  ions, 1 ppm; sorbent amount, 10 mg (a) visual color change (b) absorbance data by UV-vis.

immersed into prepared aqueous solutions and different contact times were applied between 5–25 min. According to the results, 5 min was sufficient to create a suitable color change of the synthesized ion imprinted polymer in the presence of uranyl ions.

**3.2.3. Ion-reversibility of sensing systems.** Reversible visual detection of the synthesized ion imprinted polymer nanoparticles is very sensitive to the imposed physical condition; therefore, the visual detection can be made to run either forwards or reverse by changing conditions. The reversibility of this chemosensor was tested by removal of target ions with hydrochloric acid. Then the colorimetric test was performed again. This experiment carried out several times. The color change of synthesized IIP was stable for 5 adsorption–desorption cycles. After five cycles, the recovery of the uranyl ions by the polymer was decreased according to the leach out of ligand from the IIP and memory effect of the polymer.

**3.2.4. Ion-selective sensing systems.** The selectivity of the synthesized sensor for uranyl ions was evaluated. A major advantage of the ion imprinted polymer nanoparticles as a sensor is its ability to create a selective extracting system, which prevents any interference from other components, such as anions and cations. To investigate the selectivity of ion

imprinted polymer as a sensor in the presence of potentially interfering ions coexisting with uranyl ions in wastewater and the environment, the effect of addition of various anions and cations on the recognition and removal of the sensor systems prior to the addition of 0.5 ppm concentrations of uranyl ions was individually studied at optimum pH conditions (pH of 7.0). There is a possibility for other cations to form complex with Br-PADAP, however, the size of the cavities formed in the polymer is more suitable for the uranyl ion. The cavities act as specific holes in the imprinted polymer, which allows selective adsorption of target ion. On the other hand, the cavities formed in the imprinted polymers have a specific shape and size of the template, thus they cannot not easily adsorb other interfering ions. According to the obtained results in Table 1, it could be suggested that the prepared IIP can be applied as a selective sensor for pre-concentration and visual detection of uranyl ions in the presence of other metal cations in various real samples with different complex matrices.

**3.2.5. Naked-eye colorimetric.** Fig. 8(a) displays the naked-eye colorimetric change of chemo-sensor with  $\text{UO}_2^{2+}$  ions (selected concentration). The features of the sorbent lead to the separation and pre-concentration of the ions and subsequent visual detection over a wide range [(0.001–100 ppm)] for uranyl

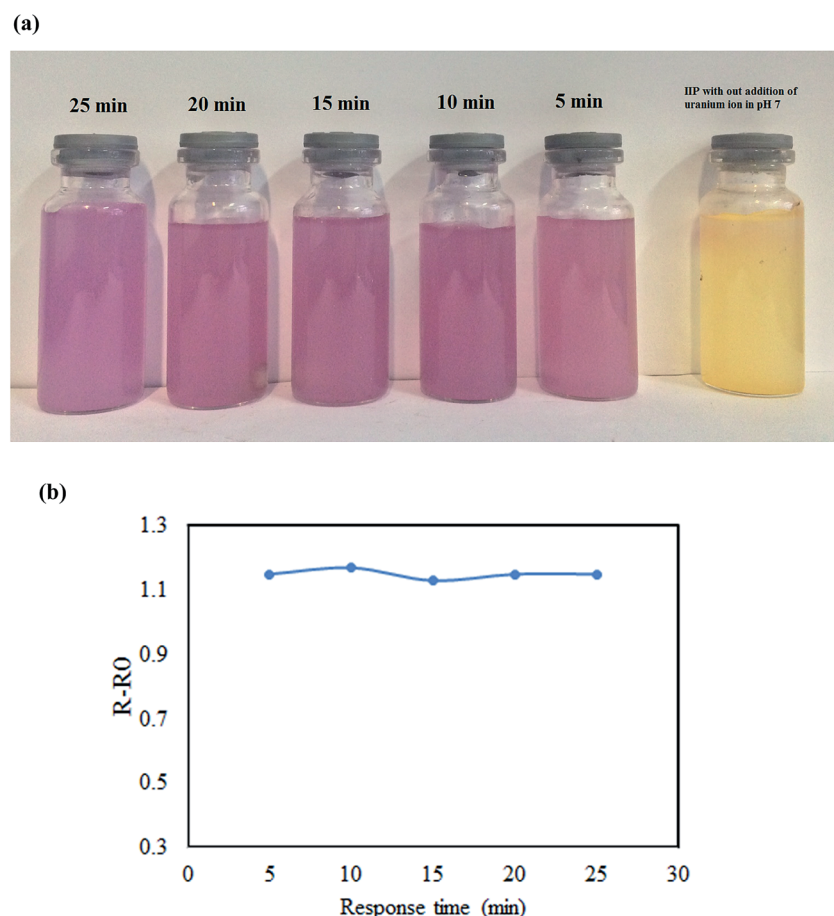


Fig. 7 Influence of response time of the ions solution on the visual detection of uranyl ions. Condition: pH of the solution, 7.0; concentration of  $\text{UO}_2^{2+}$  ions, 1 ppm; sorbent amount, 10 mg (a) visual color change (b) absorbance data by UV-vis.

**Table 1** Study the tolerance limit (TL) for interfering species of cations, during recognition of (0.5 ppm) uranyl ions using colorimetric sensor, respectively. The interfering species were added to chemo-sensor system prior to the addition of (0.5 ppm) uranyl ions at the specific conditions (amount of sorbent: 10 mg, response time: 5 min and pH of 7.0)

Tolerance limit for potentially interfering ions (ppm)

Analytes	Ca <sup>2+</sup>	Mg <sup>2+</sup>	Cu <sup>2+</sup>	Ag <sup>+</sup>	Co <sup>2+</sup>	Cd <sup>2+</sup>	Pd <sup>2+</sup>	Ni <sup>2+</sup>	Zn <sup>2+</sup>	Mn <sup>2+</sup>	Fe <sup>3+</sup>	Na <sup>+</sup>	K <sup>+</sup>
UO <sub>2</sub> <sup>2+</sup>	40	50	25	50	50	45	55	40	50	45	55	1000	1000

ions. In Fig. 8(a), a selective color change from yellow to violet with increase in concentration of uranyl ions can be observed. The color change provides a simple, rapid, and reliable method for the sensitive and selective detection of trace levels of uranyl ions without the need for sophisticated instruments.

The calibration graph is plotted for various concentrations of uranyl ions as shown in Fig. 8(b). The calibration plot was evaluated based on the relation of  $R-R_0$ , where  $R$  is the relative reflectance spectra after addition of uranyl ions and  $R_0$  is the reflectance of blank solid of the sorbent. The absorbance spectra showed a linear correlation at low concentrations of uranyl ions in the range of 0.001–1 ppm as judged from Fig. 8(b) (inset). It is also noted that the reflectance spectra were

nonlinear due to saturation effects, indicating the sensitive detection of low uranyl ions concentrations by the sorbent. This finding shows evidence of the capability of the chemo-sensor assays to determine the uranyl ions with the low concentration level. The method detection limit by the sorbent was 0.0005 ppm and this was calculated according to 3S/N (S: signal and N: noise of analysis). Therefore, the synthesized ion imprinted polymer is highly sensitive to detection uranyl ions.

**3.2.6. Real sample analysis.** To evaluate the capability of the chemo-sensor for analysis of uranyl ions in real samples (with different matrices containing various amounts of diverse ions), the method was used for the detection of uranyl ions from different samples. Table 1S (ESI†) shows the visual detection of

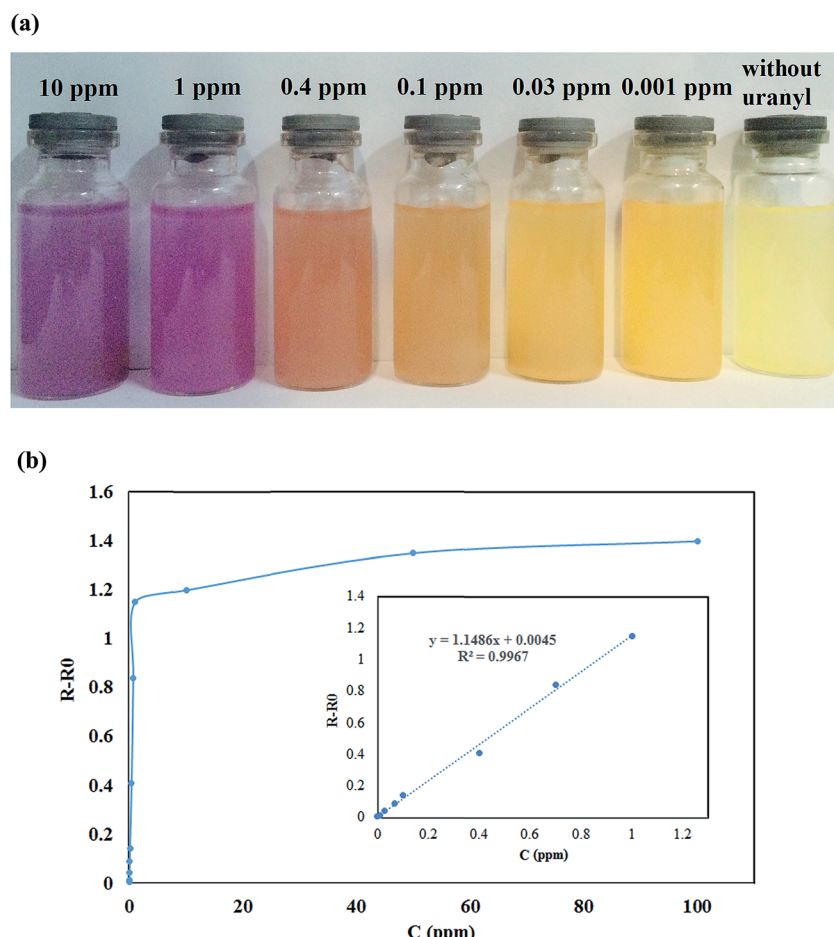


**Fig. 8** (a) The selective color change from yellow to violet with increases concentration of uranyl ions (selected concentration) (b) the calibration curve in different concentration.

**Table 2** The quantitative analysis of uranyl ions by the sensor at trace levels in spiked samples

Sample	Element	Real sample (ppb)	Added (ppb)	Found (ppb)	RR <sup>a</sup> [%]	RSD [%]
Distilled water	Uranyl	—	10.0	9.8	98.0	3.2
		—	100.0	98.2	98.2	3.8
Tap water	Uranyl	—	10.0	9.7	97.0	3.1
		—	100.0	98.5	98.5	3.5
Caspian Sea water	Uranyl	6.2	10.0	16.1	99.0	3.8
		6.2	50.0	56.5	100.6	4.2
Persian Gulf water	Uranyl	4.1	10.0	13.9	98.0	4.1
		4.1	50.0	53.8	99.4	4.5

<sup>a</sup> Relative recovery.

uranyl ions. The results clearly indicate the suitability of the synthesized chemosensor for the pre-concentration and trace visual detection of uranyl ions at trace levels in real samples.

In order to evaluate the analytical applicability of the proposed method, determination of uranyl ions in selected water samples was performed. The reproducibility of the method was demonstrated by the mean relative standard deviation (RSD). Furthermore, the relative recovery (RR) is defined as the fraction or percentage of a target analyte extracted from a sample containing a known amount of the analyte. RR calculates as following equation:

$$\text{RR (\%)} = (C_{\text{found}} - C_{\text{real}}/C_{\text{added}}) \times 100$$

where  $C_{\text{found}}$ ,  $C_{\text{real}}$ , and  $C_{\text{added}}$  are the concentrations of analyte after addition of a known amount of standard in the real sample, the concentration of analyte in real sample and the concentration of a known amount of standard, which was spiked to the real sample, respectively.

The appropriate data was found for analysis of the target ion; therefore, the prepared ion imprinted polymer can be used as a reliable sample treatment technique for trace determination of uranyl ions in water samples. The obtained data for analysis of water samples was summarized in Table 2.

**3.2.7. Adsorption capacity.** In order to study the adsorption capacity of synthesized ion imprinted polymer nanoparticles and non-imprinted polymer nanoparticles, 10 mg of each samples was added to 25 mL of solutions with 50 ppm concentration of uranyl ion at pH = 7. After shaking for 5 min, the mixture was centrifuged. The maximum adsorption capacity of the ion imprinted polymer and non-imprinted polymer for uranyl ions were 46 and 9 mg g<sup>-1</sup>, respectively.

## 4. Conclusion

To the best of our knowledge, this is the first time that the ion imprinted polymer nanoparticles were applied as a highly selective and sensitive colorimetric sensor for visual detection of uranyl ions at trace levels in aqueous solution with naked eye. Results revealed that the ion imprinted polymer sensor can be used as a simple pre-concentrator to yield high preconcentration efficiency, leading to visual detection and complete removal of uranyl ions over a wide, adjustable range of

concentrations. With our novel visual sensor, concentrations of UO<sub>2</sub><sup>2+</sup> as low as 0.001 ppm can be detected with naked eye. The designed chemo-sensor can be used as an effective, simple, rapid, reversible and reliable visual sensor for determination of uranyl ions. The prepared sorbent was characterized with different techniques such as solid state UV-vis, FT-IR, TGA, DTA, SEM and CHN analysis.

## Acknowledgements

We gratefully acknowledge financial support from the Research Council of Shahid Beheshti University.

## References

- 1 K. B. Gongalsky, *Environ. Monit. Assess.*, 2003, **89**, 197–219.
- 2 E. Schnug and B. G. Lottermoser, *Environ. Sci. Technol.*, 2013, **47**, 2433–2434.
- 3 N. Casacuberta, P. Masque, J. Garcia-Orellana, J. M. Bruach, M. Anguita, J. Gasa, M. Villa, S. Hurtado and R. Garcia-Tenorio, *J. Hazard. Mater.*, 2009, **170**, 814–823.
- 4 EPA, U.S., *EPA Integrated Risk Information System (IRIS) Electronic Database*, U.S., Environmental Protection Agency, Washington, DC, 1996.
- 5 K. Chandrasekaran, D. Karunasagar and J. Arunachalam, *Anal. Methods*, 2011, **3**, 2140–2147.
- 6 J. J. Gonzalez, D. Oropeza, X. Mao and R. E. Russo, *J. Anal. At. Spectrom.*, 2008, **23**, 229–234.
- 7 C. Moeser, R. Kautenburger and H. Philipp Beck, *Electrophoresis*, 2012, **33**, 1482–1487.
- 8 S. A. Abbasi, *Int. J. Environ. Anal. Chem.*, 1989, **36**, 163–172.
- 9 M. Mlakar and M. Branica, *Anal. Chim. Acta*, 1989, **221**, 279–287.
- 10 A. K. Brown, J. Liu, Y. He and Y. Lu, *ChemBioChem*, 2009, **10**, 486–492.
- 11 R. S. Addleman, M. Carrott, C. M. Wai, T. E. Carleson and B. W. Wenclawiak, *Anal. Chem.*, 2001, **73**, 1112–1119.
- 12 A. Safavi and M. Bagheri, *Anal. Chim. Acta*, 2005, **530**, 55–60.
- 13 Y. Luo, Y. Zhang, L. Xu, L. Wang, G. Wen, A. Liang and Z. Jiang, *Analyst*, 2012, **137**, 1866–1871.
- 14 P. T. Varineau, R. Duesing and L. E. Wangen, *Appl. Spectrosc.*, 1991, **45**, 1652–1655.

- 15 A. Becker, H. Tobias and D. Mandler, *Anal. Chem.*, 2009, **81**, 8627–8631.
- 16 R. M. Z. Kakhki and G. Rounaghi, *Mater. Sci. Eng., C*, 2011, **31**, 1637–1642.
- 17 A. M. Powe, K. A. Fletcher, N. N. Luce St, M. Lowry, S. Neal, M. E. McCarroll, P. B. Oldham, L. B. McGown and I. M. Warner, *Anal. Chem.*, 2004, **76**, 4614–4634.
- 18 O. S. Wolfbeis, *Anal. Chem.*, 2004, **76**, 3269–3283.
- 19 S. Ganesh, F. Khan, M. K. Ahmed, P. Velavendan, N. K. Pandey, U. K. Mudali and S. K. Pandey, *J. Radioanal. Nucl. Chem.*, 2012, **292**, 331–334.
- 20 D. A. Nivens, Y. K. Zhang and S. M. Angel, *J. Photochem. Photobiol., A*, 2002, **152**, 167–173.
- 21 M. Wu, L. Liao, M. Zhao, Y. Lin, X. Xiao and C. Nie, *Anal. Chim. Acta*, 2012, **729**, 80–84.
- 22 D. Pestov, C. C. Chen, J. D. Nelson, J. E. Anderson and G. Tepper, *Sens. Actuators, B*, 2009, **138**, 134–137.
- 23 J. Liu and Y. Lu, *Angew. Chem., Int. Ed.*, 2007, **46**, 7587–7590.
- 24 J. Li and Y. Lu, *J. Am. Chem. Soc.*, 2000, **122**, 10466–10467.
- 25 N. Rupcich, W. Chiuman, R. Nutiu, S. Mei, K. K. Flora, Y. F. Li and J. D. Brennan, *J. Am. Chem. Soc.*, 2006, **128**, 780–790.
- 26 J. Liu, A. K. Brown, X. Meng, D. M. Cropek, J. D. Istok, D. B. Watson and Y. Lu, *Proc. Natl. Acad. Sci. U. S. A.*, 2007, **104**, 2056–2061.
- 27 T. Prasada Rao, R. Kala and S. Daniel, *Anal. Chim. Acta*, 2006, **578**, 105–116.
- 28 M. Behbahani, M. Taghizadeh, A. Bagheri, H. Hosseini, M. Salarian and A. Tootoonchi, *Microchim. Acta*, 2012, **178**, 429–437.
- 29 L. Zhoua, C. Shanga, Z. Liua, G. Huanga and A. A. Adesinab, *J. Colloid Interface Sci.*, 2012, **366**, 165–172.
- 30 S. Shirvani-Arania, S. J. Ahmadi, A. Bahrami-Samani and M. Ghannadi-Maragheh, *Anal. Chim. Acta*, 2008, **623**, 82–88.
- 31 B. Godlewska-Zyłkiewicz, B. Lésniewska and I. Wawreniuk, *Talanta*, 2010, **83**, 596–604.